Journal of ELECTRONIC MATERIALS, Vol. 50, No. 4, 2021
https://doi.org/10.1007/s11664-020-08478-z

ASIAN CONSORTIUM ACCMS–INTERNATIONAL CONFERENCE ICMG 2020

First-Principles Simulation of Structural, Electronic and Optical Properties of Cerium Trisulfide (Ce_2S_3) Compound

R.M. ARIF KHALIL,[1,6] MUHAMMAD IQBAL HUSSAIN,[1,2] MUHAMMAD IMRAN,[3] FAYYAZ HUSSAIN,[1,7] NYLA SAEED,[1] G. MURTAZA,[4] ANWAR MANZOOR RANA,[1] and CHANDRESWAR MAHATA[5]

1.—Materials Simulation Research Laboratory (MSRL), Department of Physics, Bahauddin Zakariya University, Multan 60800, Pakistan. 2.—Department of Physics, University of Education, Lahore 54000, Pakistan. 3.—Department of Physics, Govt. College University Faisalabad, Faisalabad, Pakistan. 4.—Centre for Advanced Studies in Physics, G. C. University Lahore, Lahore, Pakistan. 5.—School of Electronics Engineering, Chungbuk National University, Cheongju 28644, South Korea. 6.—e-mail: muhammadarif@bzu.edu.pk. 7.—e-mail: fayyazhussain248@yahoo.com

In this work, the structural, electronic and optical properties of Ce_2S_3 compound have been explored using CASTEP simulation code. We explore the crystal structure, lattice parameters, electronic band structure, the total density of states (TDOS), the partial density of states (PDOS) and the optical functions of the Ce_2S_3 compound using first-principles simulation based on density functional theory (DFT). The orthorhombic crystal structure with space group (*Pnma*) of Ce_2S_3 is stable both chemically and structurally. The lattice parameters of this compound are obtained by the optimization method. The lattice parameters measured in this study (a = 7.53 Å, b = 4.10 Å and c = 15.73 Å) indicate excellent agreement with experimental and previous theoretical results. The electronic properties are investigated using Perdew–Burke–Ernzerhof generalized gradient approximation (PBE-GGA) and GGA observe U approaches within DFT employing CASTEP code. The energy bandgap value reported in this study (E_g = 0.76 eV) is comparable to the previous theoretical value. This energy bandgap value shows that Ce_2S_3 belongs to the semiconductor category. The frequency-dependent dielectric function and some optical properties such as reflectivity, absorption coefficient, optical dielectric constant, optical conductivity and the energy loss function have also been calculated in the present work. The optical reflectivity is noted to be maximum in the ultraviolet region of the electromagnetic spectrum.

Key words: Crystal structure, electronic bandgap, Ce_2S_3 compound, PBE-GGA, optical properties

INTRODUCTION

Eastman et al.[1] and Flahaut et al.[2] reported that sesquisulfide compounds (e.g. Ce_2S_3) have more than one phase. Ce_2S_3 exists as α, β and γ phases, and researchers are attracted to them because of their superior physical, thermal, mechanical and electronic properties, together with better optical

(Received June 17, 2020; accepted September 9, 2020; published online October 6, 2020)

stability and electrical conductivity.[3–5] However, tremendous efforts have been made to synthesize different phases of Ce_2S_3 for several applications.

The color and structure of the three phases are described as follows: α-Ce_2S_3 has an orange or black/brown color and orthorhombic structure, β-Ce_2S_3 possesses a burgundy color and tetragonal structure and γ-Ce_2S_3 appears in dark red with a cubic structure. A literature review[6–9] revealed that the α, β and γ phases occur at temperatures of < 900 °C, > 900 °C and > 1200 °C, respectively. Many misperceptions still exist about the allotropes of cerium sesquisulfide and about their transformation temperatures.

Inorganic colorants have been used ubiquitously for decoration purposes, especially red pigments. But the use of traditional red colorants is restricted, unfortunately, because these have heavy metals such as Cd, Cr and Pb, and they are dangerous for both the environment and human health. Because of its outstanding weather resistance, dispersion and safety properties, the γ-phase of the Ce_2S_3 compound has been used to replace these traditional red inorganic colorants and has become a source of interest for many researchers.[10–12] As γ-Ce_2S_3 is an environmentally friendly colorant and has outstanding colorant performance,[13] it is very suitable for use in plastics, paints and coatings.

γ-Ce_2S_3 is also suitable for application in polypropylene, which is an extensively used plastic. Ding et al.[14] suggest the use of rare-earth sulfides as colorant in polydimethylsiloxane. Although these works are very helpful for investigating the applications of γ-Ce_2S_3 in some plastics, compounds such as polyvinyl chloride (PVC) and polyethylene (PE) are rarely reported. That is why researchers are investigating the coloring properties of the γ-phase for both PVC and PE.[15]

For processing molten metals, cerium sesquisulfide (Ce_2S_3) can be used as a crucible material. Because its thermal expansion coefficient is low, it is stable at high temperatures and also has good stability in air. Ce_2S_3 compound and the other sulfides of cerium exhibit low reactivity to molten metals that are very reactive, like actinides and alkali metals.[12] Because of the low reactivity between the metals and crucible, these crucibles are not damaged and are reusable, thereby decreasing expenses and environmental waste by replacing damaged or corroded crucibles. The properties of Ce_2S_3 compounds have made it a particularly worthy material for use in crucibles for processing alkali metals.[16,17]

Before this work, no theoretical study for structural, electronic and optical properties of Ce_2S_3 compound is reported by using the CASTEP code. The present study is performed to compare the role of Perdew–Burke–Ernzerhof generalized gradient approximation (PBE-GGA) and GGA+U functionals for this material. As very little experimental work has been done for the optical properties of cerium trisulfide compound, this study provides a deep understanding of Ce_2S_3 compounds with regard to their structural, electronic and optical properties.

RESEARCH METHODOLOGY

In the present density functional theory (DFT)-based study, the structural and optoelectronic properties for the α-phase of Ce_2S_3 are investigated using CASTEP code[18] through PBE-GGA along with the GGA+U approaches. In particular, the norm-conserving pseudopotential produced by the CASTEP package with the Perdew–Burke–Ernzerhof approach[19] is utilized for the determination of exchange correlation potential. In order to explain the equations of the Kohn–Sham theorem,[20] the conjugate gradient method[21] is utilized. In this work, the total energy of the system is found to converge within 1 meV, while a cutoff energy of 550 eV is adopted for the considered compounds. These total energy calculations are performed using a $6 \times 10 \times 2$ Monkhorst–Pack grid[22] for optimization and exploration of the structural properties and estimation of the electronic bandgap. For electronic wave functions, plane-wave (PW) basis sets are used. For cerium atoms, $4f^1\ 5s^2\ 5p^6\ 5d^1\ 6s^2$ electrons and $3s^2\ 3p^4$ for electrons of sulfur atoms are considered as pseudo-electrons. The GGA+U functional is also adopted to calculate the optical properties. The Hubbard parameter "U" is adopted with a magnitude of 6 eV for each Ce atom to contribute to the repulsive coulombic potential for f electrons for the calculation of electronic and optical properties.

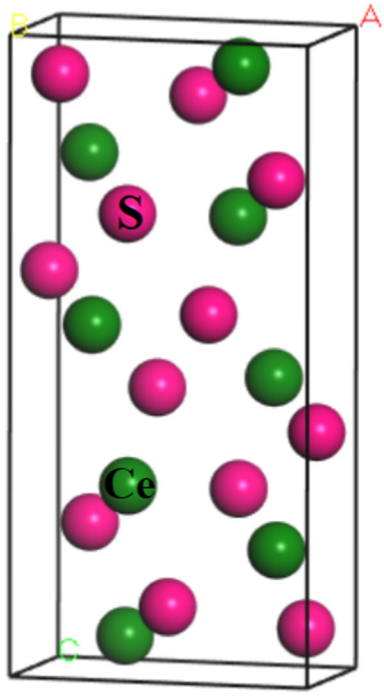

Fig. 1. Crystal structure of α-Ce_2S_3 compound.

RESULTS AND DISCUSSION

Structural Properties

The crystal structure of the α-phase of Ce_2S_3 is shown in Fig. 1. In this crystal structure, the eight green-colored atoms represent cerium, while the remaining 12 yellow-colored atoms indicate sulfur. The crystal structure of the α-Ce_2S_3 compound is orthorhombic ($PbCl_2$-type structure), which possesses a *Pnma* space group (no. 62) with a D_{2h} point group. We explored the lattice parameters of α-Ce_2S_3 and compared our results with previous theoretical and experimental studies, which are illustrated in Table I. It was found that our results and previous theoretical work[23] deviate by only 2%. Interestingly, the magnitudes of lattice parameters computed in the present study are found to replicate the lattice parameters determined experimentally as reported by Schleid et al.,[24] which are also summarized in Table I. These reported results are useful for the estimation of all physical properties of this compound. The main purpose of the present work is to perform a complete DFT-based study to explore the structural properties of the Ce_2S_3 compound.

Electronic Properties

In this theoretical work, an ab initio study is conducted using a semi-local exchange correlation approximation to determine the electronic properties of α-Ce_2S_3. PBE-GGA and GGA+U approaches are investigated to determine the energy bandgap, electronic density of states (eDOS) and partial density of states for the Ce_2S_3 compound. The band structure and electronic density of states using a PBE-GGA approach are shown in Fig. 2a and b. The partial density of states are presented in Fig. 3 to determine the contribution at the elemental level of the electronic states in the conduction mechanism. It can be observed from Fig. 2a and b that when the PBE-GGA functional is used, few valence states are available in the forbidden region. as these states have crossed the Fermi level, indicating that the considered compound behaves as a metallic material. Likewise, a similar trend is seen in Fig. 3. However, contrary to the results of the PBE-GGA, a significant energy bandgap value of 0.76 eV is observed in Fig. 4 a and b, which represents the band structure in comparison to the electronic density of states of the considered compounds when using the advanced GGA+U functional. It is well known that the GGA+U functional is an appropriate method to account for the *f*-state electrons of an element such as cerium, since by adding the Hubbard potential U, a shift of energy states is observed from the valence band toward the conduction band, leaving a gap between them. This makes the compound a semiconducting material. Such behavior of the *f*-state electrons was ignored by the PBE-GGA when calculating the energy bandgap and electronic density of states.

As shown in Fig. 4, the electronic band structure verifies that Ce_2S_3 belongs to a semiconductor category, since a direct gap value of 0.76 eV is observed at point G, and since the top of the valence band and bottom of the conduction band are connected at the G point (Fig. 4). Our calculated electronic bandgap of 0.76 eV using CASTEP code, as given in Table I, is found to be quite comparable to that determined by earlier theoretical study[23] using VASP code. Moreover, the electronic band structure and density of states also depict excellent agreement with the results of Windiks et al.[23]

The calculated partial density of states using the GGA+U functional are presented in Fig. 5. It can be seen that the *s*-states of the considered compound participate significantly only in the valence band formation away from the Fermi level at about −11 eV, whereas *p*-states demonstrate their major role in the valence band near the Fermi level as well as at −18 eV. As regards *d*- and *f*-states, it can be seen that these states have contributions across the Fermi level, with a significant energy bandgap of 0.76 eV, and play a major role in the formation of the conduction band. These two states are thus very important for the conduction mechanism, while *p*-states show minimal contribution to conduction band formation.

The spin-polarized total density of states for the Ce_2S_3 compound calculated using the GGA+U functional are shown in Fig. 6, wherein the blue line indicates the spin-up↑ channel and the red line represents the spin-down↓ channel. A Hubbard parameter "U" of 6 eV is adopted for each Ce atom to contribute to the repulsive coulombic potential caused by *f*-state electrons. This figure further reveals that spin-up↑ and spin-down↓ states do not depict symmetry, which means that the two spin channels↑↓ are not replicas of each other, leading to

Table I. Summary of the lattice parameters and energy bandgap of the α-Ce_2S_3 compound

Compound	Reference	Lattice constant (Å)			Energy bandgap E_g (eV)
		a	*b*	*c*	
Ce_2S_3	Present work	7.53	4.10	15.73	0.76
	Theoretical work[23]	7.56	4.12	15.73	0.80
	Experimental work[24]	7.53	4.10	15.73	

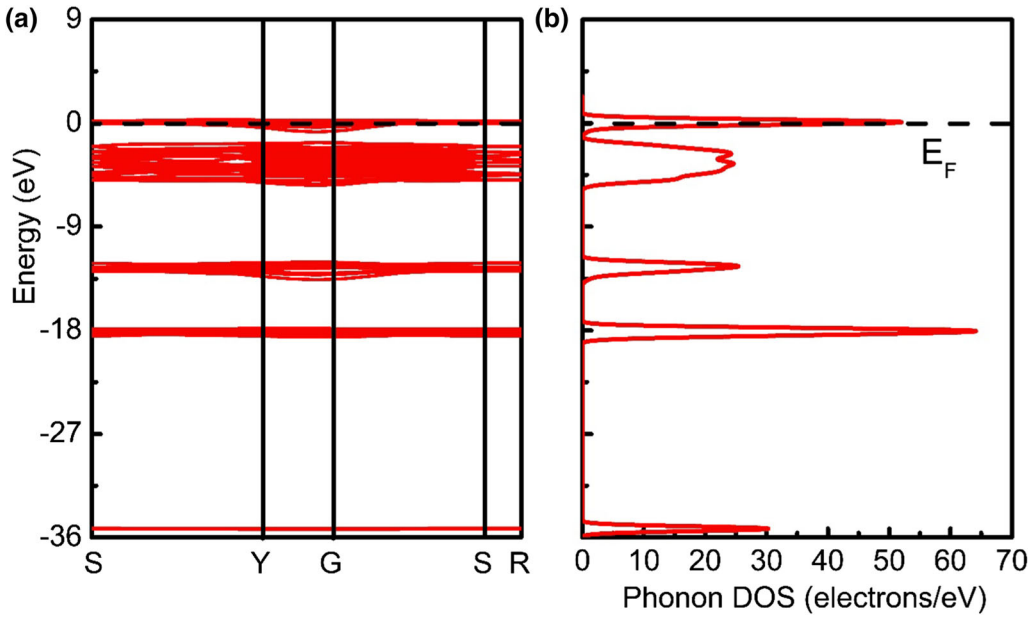

Fig. 2. (a) Calculated electronic band structure and (b) eDOS for the α-phase of Ce_2S_3 compound using the PBE-GGA functional.

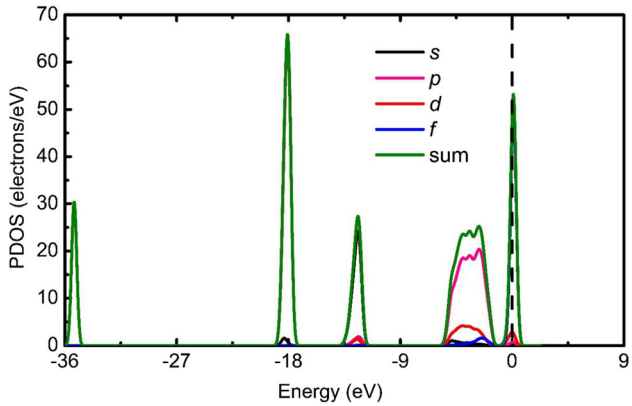

Fig. 3. Calculated partial density of states (PDOS) of Ce_2S_3 using the PBE-GGA functional.

the fact that there exists magnetic domains with a suitable net magnetic field; therefore, it can be concluded that the considered compound (Ce_2S_3) falls within the ferromagnetic category of materials. The magnetic moment of each Ce atom is noted to be 1 μ_B. These calculated spin-polarized densities of states also support the viewpoint that a sufficient energy gap (0.76 eV) exists between conduction and valence states when calculations are performed through a GGA+U approach.

Optical Properties

Optical analysis of the Ce_2S_3 compound is essential for further interpretation of the electronic band structure. In this work, Gaussian smearing is fixed at 0.5 eV for fine-tuned calculations of the optical properties. The optical functions of Ce_2S_3 are explored by the frequency-dependent dielectric constant as expressed below:

$$\varepsilon(\omega) = \varepsilon_1(\omega) + i\varepsilon_2(\omega). \tag{1}$$

Equation 1 has a close relation to the band structure. The real and imaginary parts of the dielectric functions are interlinked by the well-known Kramer–Kronig relation, which is expressed as[25–29]:

$$\varepsilon_2(\omega) = \frac{Ve^2}{2m^2\omega^2}\sum_{ij}\int k_i|p|k_j^2 f(k_i)\left(1-f\left(k_j\right)\right) \delta\left(E_{k_i}-E_{k_j}-\omega\right)d^3k \tag{2}$$

$$\varepsilon_1(\omega) = 1 + \frac{2}{\pi}P\int_0^\infty \frac{\omega'\varepsilon_2(\omega)}{\omega'^2-\omega^2}\mathrm{d}\omega. \tag{3}$$

The reflectivity can be achieved directly from Fresnel's formula as expressed below:[30]

$$R(\omega) = \left|\frac{\sqrt{\varepsilon(\omega)}-1}{\sqrt{\varepsilon(\omega)}+1}\right|^2. \tag{4}$$

Other optical parameters including the absorption spectrum $\alpha(\omega)$, loss function $L(\omega)$, real part of conductivity and refractive index $n(\omega)$ are calculated from the equations given in Zhang et al.:[31]

$$\alpha(\omega) = \frac{\omega}{c}\sqrt{2\left(\sqrt{\varepsilon_1^2(\omega)+\varepsilon_2^2(\omega)}-\varepsilon_1(\omega)\right)} \tag{5}$$

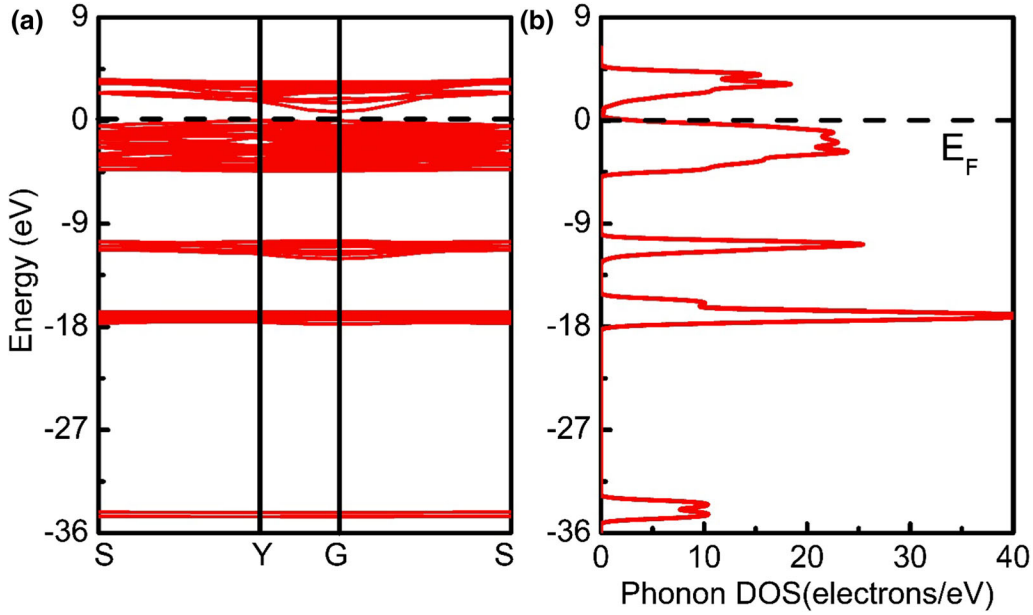

Fig. 4. (a) Calculated electronic band structure and (b) DOS for the α-phase of Ce_2S_3 compound using the GGA+U functional.

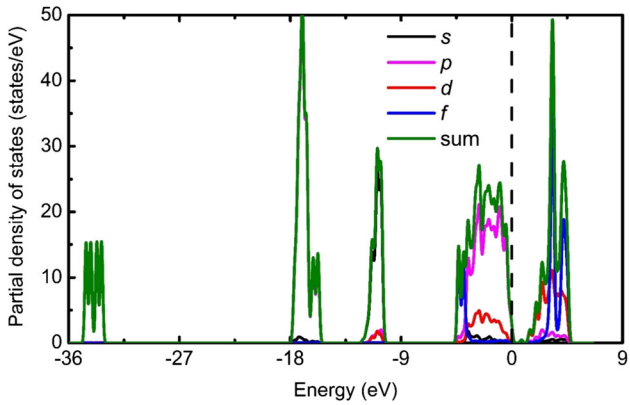

Fig. 5. Calculated partial density of states of Ce_2S_3 using the GGA+U functional.

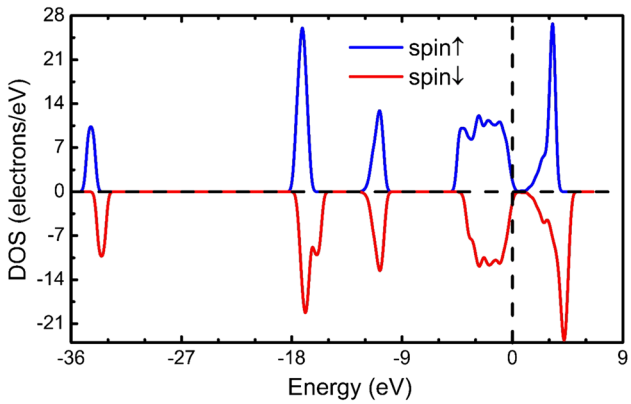

Fig. 6. Calculated spin-polarized total density of states using the GGA+U functional for Ce_2S_3 (Color figure online).

$$n(\omega) = \sqrt{\frac{\sqrt{\varepsilon_1^2(\omega) + \varepsilon_2^2(\omega)} + \varepsilon_1(\omega)}{2}} \tag{6}$$

$$k(\omega) = \sqrt{\frac{\sqrt{\varepsilon_1^2(\omega) + \varepsilon_2^2(\omega)} - \varepsilon_1(\omega)}{2}} \tag{7}$$

$$L(\omega) = \frac{\varepsilon_2(\omega)}{\varepsilon_1(\omega) + \varepsilon_2(\omega)} \tag{8}$$

The fundamental optical parameters of the Ce_2S_3 compound are investigated within a frequency range from 0 to 20 eV, and particularly, dielectric functions are illustrated in Fig. 7a. It is reported that the real component of the dielectric function displays light polarization, while the imaginary dielectric function exhibits the absorption of light on the surface of a material. Figure 7 illustrates that initially, the real part of the dielectric function of Ce_2S_3 starts increasing from the critical value, then drops to zero value at a photon energy of 4.8 eV. This, however, extends toward the negative region, depicting metallic behavior during the specific range of photon energy, i.e., from 4.8 eV to 9.0 eV, wherein polarization is found to be lowest but absorption is highest, as displayed in Fig. 7b. Contrary to the former case, it has been observed that the magnitude of the imaginary dielectric function remains zero up to the value of the energy

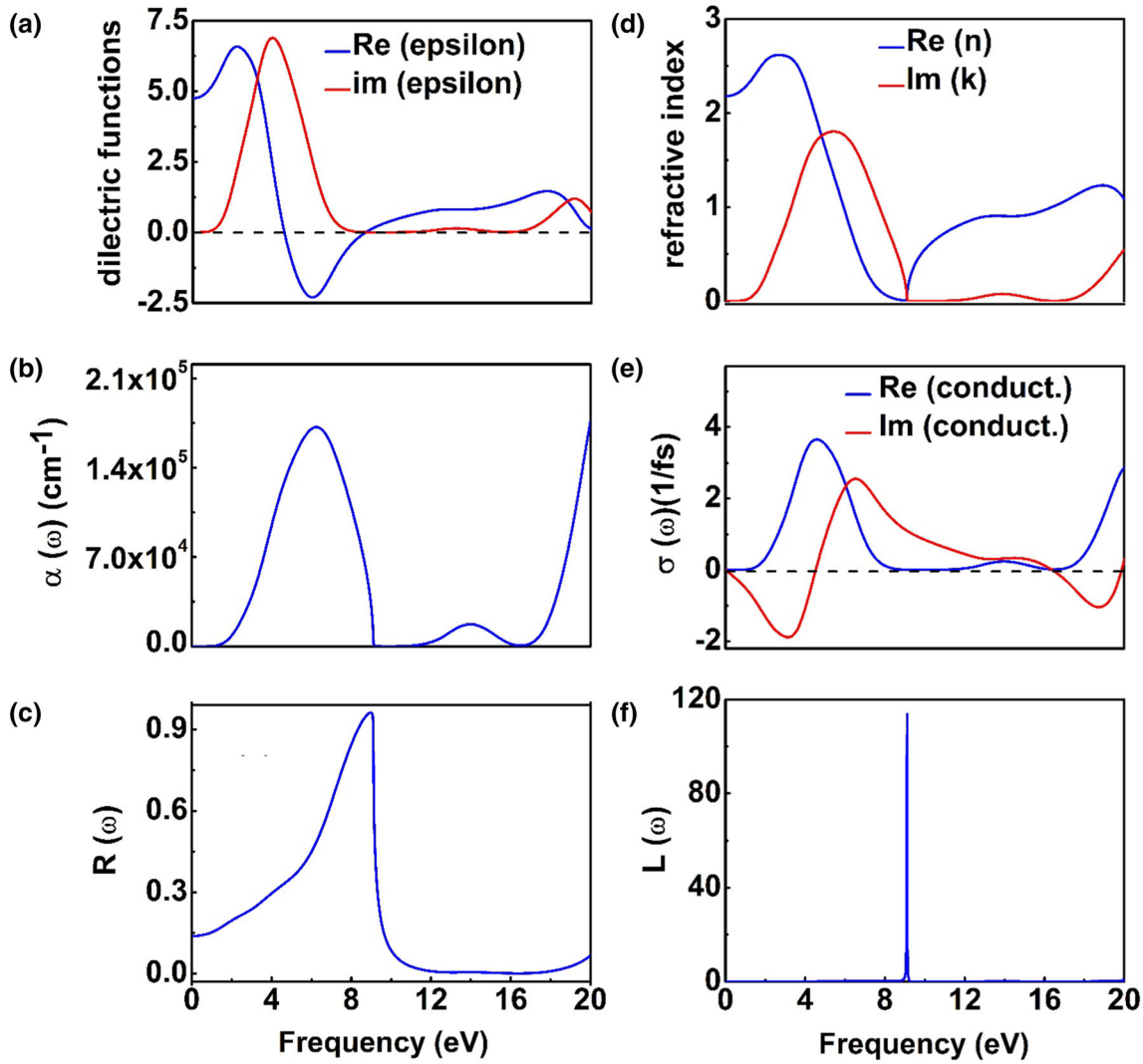

Fig. 7. Plots of calculated data: (a) dielectric function, (b) absorption coefficient, (c) reflectivity $R(\omega)$, (d) refractive index and extinction coefficient, (e) optical conductivity $\sigma(\omega)$ and (f) energy loss function $L(\omega)$ of Ce_2S_3.

bandgap of the considered compound. Then $\varepsilon_2(\omega)$ raises its flight and approaches a maximum value, indicating the highest absorption at an energy value of 4.25 eV. Thereafter, the imaginary part of the dielectric function descends to zero values at 8.34 eV. In a higher energy range, both components of the dielectric function become approximately parallel to the energy axis, with slight variations occurring due to different rates of inner band transitions.

The absorption spectrum of Ce_2S_3 is shown in Fig. 7b, in which maximum absorption occurs in the visible range of the electromagnetic radiation. This indicates that Ce_2S_3 is a good absorptive material. Figure 7b shows that absorption rises from zero to the maximum value at energy of 6.36 eV, where the dispersion of light is very small. In the region of higher energy, the fluctuation in absorption peaks indicates the different inter-band transition rates, and finally, no light is absorbed by a material due to the metallic behavior of the investigated compound. Figure 7c demonstrates the reflectivity spectrum of the Ce_2S_3 compound with respect to frequency (eV). Due to the reflection of photons at various incident angles from the surface of Ce_2S_3, only a single broad peak is detected in the frequency range of 0–20 eV, as shown in Fig. 7c. The highest peak indicates that reflectivity is greatest (0.95) at a frequency value of 8.97 eV in the ultraviolet range, after which reflectivity starts to decrease at a higher frequency.

The refractive index $n(\omega)$ is a dimensionless number that can express how light radiation spreads through a specified optical medium. To design optoelectronic devices, the complex refractive index and extinction coefficient are very important. The refractive index and extinction coefficient for the Ce_2S_3 compound are shown in Fig. 7d. For cerium trisulfide, the value of $n(0)$ is 2.18. Two broader peaks are observed: one for the real part showing the transparency of this compound, and the

other for the extinction coefficient describing the absorption of light rays. The refractive index starts to decrease from 3.0 eV and approaches zero at an energy of 9.14 eV, wherein the transparency is seen to be very small with approximately maximum absorption. Extinction coefficient $k(\omega)$ shows that the absorption of electromagnetic radiation remains zero until the bandgap energy; however, after the threshold frequency, the maximum absorption peak is attained. The imaginary refractive index exhibits one main peak at an energy of 5.56 eV. The analysis of the optical refractive index indicates that the absorption or extinction coefficient is high in the ultraviolet region.

The real and imaginary parts of the optical conductivity of cerium trisulfide are shown in Fig. 7e. In this plot, two sharp peaks are detected: one for the real conductivity and the other for imaginary conductivity. The real conductivity is highest at energy of 4.60 eV. Figure 7e shows that the imaginary part of the optical conductivity is greatest at an energy value of 7.16 eV in the ultraviolet region.

Figure 7f is a plot of the energy loss function with respect to frequency for Ce_2S_3. It defines the loss of energy when fast-moving electrons move across the material from the top of the valence band to the bottom of the conduction band. A prominent peak is observed at 9.14 eV, which is associated with the sudden decrease in reflectivity in this energy range. This energy-loss spectrum indicates an intense maximum at about 9.14 eV due to plasmon excitation.

CONCLUSIONS

In the present work, the structural, electronic and optical properties of a Ce_2S_3 compound are reported using PBE-GGA and GGA+U approaches within the density functional theory (DFT). The lattice parameters calculated in this work are a = 7.53 Å, b = 4.10 Å and c = 15.73 Å, which indicate that $\sim$ 2% deviation has occurred as compared to the experimental result and 0.5% deviation from the previous theoretical result due to different approaches used for calculations. The band structure calculations show that the α-Ce_2S_3 compound is a semiconductor with a direct bandgap value of 0.76 eV. Moreover, we have investigated the optical functions (absorption coefficient, reflectivity, real and imaginary dielectric function, conductivity, refractive index and energy loss function). From the absorption spectrum, a high value of absorption is observed in the ultraviolet region of the electromagnetic radiation. The spin DOS calculations show that the Ce_2S_3 compound is a ferromagnetic material.

REFERENCES

1. E.D. Eastman, L. Brewer, L.A. Bromley, P.W. Gilles, and N.L. Lofgren, *J. Am. Chem. Soc.* 72, 2248 (1950).
2. J. Flahaut and M. Guittard, *Comptesrendus* 243, 1419 (1956).
3. T. Takeshita, K.A. GschneidnerJr, and B.J. Beaudry, *J. Appl. Phys.* 57, 4633 (1985).
4. C.M. Forster and W.B. White, *J. Am. Ceram. Soc.* 80, 273 (1997).
5. C.M. Forster and W.B. White, *Mater. Res. Bull.* 41, 448 (2006).
6. J.M. Tomczak, L.V. Pourovskii, L. Vaugier, A. Georges, and S. Biermann, *PNAS* 110, 904 (2012).
7. H.M. Smith, eds., *High Performance Pigments*, Vol. 4 (Darmstadt: Wiley-VCH, 2002), p. 27.
8. I.A. Kariper, *Prog. Nat. Sci. Mater. Int.* 24, 663 (2014).
9. I.A. Kariper, *Mater. Res.* 20, 1345 (2017).
10. S. Roméro, A. Mosset, P. Macaudière, and J.C. Trombe, *J. Alloys Compd.* 302, 118 (2000).
11. F. Marrot, A. Mosset, J.C. Trombe, P. Macaudière, and P. Maestro, *J. Alloys Compd.* 259, 145 (1997).
12. S. Hirai, K. Shimakage, Y. Saitou, and L. Brewer, *J. Am. Ceram. Soc.* 81, 145 (1998).
13. P. Maestro and D. Huguenin, *J. Alloys Compd.* 225, 520 (1995).
14. Y. Ding, J. Gu, T. Zhang, A.X. Yin, L. Yang, Y.W. Zhang, and C.H. Yan, *JACS* 134, 3255 (2012).
15. W. Dongri, Z. Yongqing, and Y. Shiyong, *J. Rare Earths* 35, 1042 (2017).
16. P. Hogan, High Temperature Synthesis of Sulphides of Cerium and Thermodynamic System Modeling, Master Thesis, University of Florida, 2002.
17. K. Gibbard, High Temperature Syntesis of Cerium Sulphides and Kinetic Modeling, Master of Science Thesis, University of Florida, 2005.
18. S.J. Clark, M.D. Segall, C.J. Pickard, P.J. Haspani, P.J.H. Matt, K. Refson, M.C. Pyne, and Z. Kristallogr, *Cryst. Mater.* 220, 567 (2005).
19. J.P. Perdew, K. Burke, and M. Ernzerhof, *Phys. Rev. Lett.* 77, 3865 (1996).
20. W. Kohn and L.J. Sham, *Phys. Rev.* 140, A1133 (1965).
21. M.C. Payne, M.P. Teter, D.C. Allan, T.A. Arias, and J.D. Joannopoulos, *Rev. Mod. Phys.* 64, 1045 (1992).
22. H.J. Monkhorst and J.D. Pack, *Phys. Rev. B* 13, 5188 (1976).
23. R. Windiks, E. Wimmer, L. Pourovskii, S. Biermann, and A. Georges, *J. Alloys Compd.* 459, 438 (2007).
24. T. Schleid and P. Lauxmann, *J. Inorg. G. Chem.* 625, 1053 (1999).
25. D.C. Ambrosch and J.O. Sofo, *Comput. Phys. Commun.* 175, 1 (2006).
26. M. Fox, *Optical Properties of Solids* (Oxford: Oxford University Press, 2001).
27. F. Wooten, *Optical Properties of Solids* (London: Academic Press, 1972).
28. H. Wang, Y.F. Wang, X.W. Cao, L. Zhang, M. Feng, and G.X. Lan, *Phys. Stat. Sol. B.* 246, 437 (2009).
29. S. Saha and T.P. Sinha, *Phys. Rev. B.* 62, 8828–8834 (2000).
30. A. Radzwan, R. Ahmed, A. Shaari, A. Lawal, Y. N. Malays, J. Fundam, *Appl. Sci.* 13, 285 (2017).
31. X. Zhang, D. Rao, R. Lu, K. Deng, and D. Chen, *AIP Adv.* 5, 057111 (2015).